KCNC3 as a prognostic indicator and a predictive marker for immunotherapy in colorectal cancer

Quanqing Li[1#], Jiaying Lv[1,2#], Hongxia Duan[3], Pingping Sun[2], Bing Lu[2], Wenyu Shi[1,3], Yihong Cai[3]

[1]Department of Oncology, Affiliated Hospital of Nantong University, Nantong, China; [2]Department of Clinical Biobank, Affiliated Hospital of Nantong University, Nantong, China; [3]Department of Chemotherapy, Affiliated Hospital of Nantong University, Nantong, China

Contributions: (I) Conception and design: Y Cai, Q Li, W Shi; (II) Administrative support: Y Cai, W Shi; (III) Provision of study materials or patients: J Lv, H Duan; (IV) Collection and assembly of data: P Sun, B Lu; (V) Data analysis and interpretation: Q Li, P Sun; (VI) Manuscript writing: All authors; (VII) Final approval of manuscript: All authors.

[#]These authors contributed equally to this work.

Correspondence to: Yihong Cai, PhD. Department of Chemotherapy, Affiliated Hospital of Nantong University, No. 20 Xisi Road, Nantong 226000, China. Email: caiyihong@126.com; Wenyu Shi, PhD. Department of Oncology, Affiliated Hospital of Nantong University, No. 20 Xisi Road, Nantong 226000, China; Department of Chemotherapy, Affiliated Hospital of Nantong University, No. 20 Xisi Road, Nantong 226000, China. Email: shiwenyu@hotmail.com.

Background: Colorectal cancer (CRC) is a heterogeneous disease that is associated with several genetic or somatic mutations. Cancer immunotherapy has become a novel and revolutionary method of treatment for patients with advanced tumors. However, effective biomarkers that can reflect the response of CRC patients to immunotherapy have still not been identified. Our study aimed to explore the expression and functional role of KCNC3 in CRC.

Methods: The correlation between KCNC3 expression levels and CRC progression was explored and validated using data from The Cancer Genome Atlas (TCGA) and patient's samples from the Affiliated Hospital of Nantong University. Univariate and multivariate Cox regression models were developed to determine the predictive value of KCNC3 on the prognosis and immune activation of patients with CRC. We predicted the immunotherapy response in both the high and low KCNC3 expression subgroups. Finally, we confirmed that KCNC3 promotes the proliferation and invasion of colon cancer cells.

Results: In this study, data from TCGA database and clinical patient parameters showed that high KCNC3 expression was associated with tumor immune infiltration and poor prognosis of CRC. KCNC3 expression was positively correlated with the infiltration levels of CD4^{+} cells, regulatory T cells (Tregs), and myeloid-derived suppressor cells (MDSCs), which contributed to the formation of an immunosuppressive tumor microenvironment (TME). The high expression of KCNC3 was accompanied by the upregulation of immune checkpoint molecules, including PDCD1, LAG3, FOXP3, and CTLA4, which stimulated tumor cells to evade immune surveillance. *In vitro* experiment, KCNC3 knockdown inhibited the growth and metastasis of SW1116 cells.

Conclusions: This study demonstrated that the high expression of KCNC3 contributes to the growth and invasion of CRC and confers with immunosuppressive microenvironment that can promote tumor progression and can be used to predict the poor clinical outcome of CRC patients.

Keywords: KCNC3; colorectal cancer (CRC); tumor immune microenvironment; prognosis

Introduction

Colorectal cancer (CRC), the most common type of tumor of the gastrointestinal system, is the third most common malignancy worldwide following lung and breast cancer (1). Although the mortality rate of CRC has declined, CRC still leads to a high level of mortality (2). CRC is a heterogeneous disease that involves multiple gene alterations and pathways in its pathogenesis (3). Many factors can contribute to the pathogenesis of CRC, such as the activation of oncogenes, restraint of tumor suppressors, diet, epigenetic alterations, and the abnormal activity of multiple cellular signaling pathways. The three major pathogenic mechanisms of CRC include chromosomal instability (CIN), microsatellite instability (MSI), and the CpG island methylator phenotype (CIMP) (4). Despite advancements in diagnostic techniques and comprehensive therapy, the 5-year survival rate of patients who receive surgery for colon cancer is still not satisfactory (5). Even if the residual tumor cells are subjected to standard postoperative radiotherapy and chemotherapy, their complete elimination is difficult. Early detection, intervention, and treatment are recommended to reduce morbidity and mortality (6). Early detection is difficult due to the lack of sufficient biomarkers to determine diagnosis and prognosis, which has prevented clinicians from adopting

---

Highlight box

Key findings
- KCNC3 acts as a promoter to the growth and invasion of colorectal cancer (CRC) and confers with immunosuppressive microenvironment that can promote tumor progression and can be used to predict the poor clinical outcome of CRC patients.

What is known and what is new?
- KCNC3 is a well-known oxygen-sensitive channel that has been reported less frequently in tumors.
- KCNC3 is first mentioned as a promoter to CRC. The Cancer Genome Atlas database and clinical patient parameters showed that high KCNC3 expression was associated with tumor immune infiltration and poor prognosis of CRC. *In vitro* experiment, KCNC3 knockdown inhibited the growth and metastasis of SW1116 cells.

What is the implication, and what should change now?
- KCNC3 may be a novel effective indicator for predicting the diagnostic value, prognosis, and immune response of patients with CRC.
- In future studies, we will strive to more comprehensively elucidate the mechanisms by which KCNC3 affects the prognosis of CRC patients.

---

effective methods of treatment for patients with CRC (7). The identification and development of suitable biomarkers could improve CRC diagnosis, prognosis prediction, and provide a novel therapeutic option for this subset of patients.

Immunotherapy is considered to be first-line in various tumors for good efficacy. However, its impact on colorectal treatment has been observed only in a small fraction of patients because of poor immune infiltration (8). It has been increasingly recognized that immune cell subtypes that are found within the tumor microenvironment (TME) of CRC have potential use in predicting prognosis and the treatment response (9). T-cell infiltration may have tremendous prognostic value in CRC (10). Programmed death-ligand 1 (PD-L1), programmed death-ligand 2 (PD-L2), cytotoxic T lymphocyte-associated protein 4 (CTLA4), and lymphocyte activation gene 3 (LAG3) (CD223) are inhibitory immune checkpoints which can be expressed in tumor, immune, endothelial, and muscle cells. It has been shown that LAG3 mainly performs its inhibitory function by interacting with ligands such as MHC-II or FGL1 (11). After immune ligands connect to activated lymphocytes, the adaptive anti-tumor immune responses may be attenuated, leading to the hijacking of intrinsic immune checkpoint mechanisms. A recent study reported that the expression of immune checkpoint markers [e.g., CTLA4, programmed death-1 (PD-1), PD-L1, and LAG3 targeted by immunotherapy] in CRC may tip the balance of the antitumor effect between T helper (Th)1 and cytotoxic T lymphocyte (CTL) immune response, especially in MSI CRC (12). Recent evidence indicates that PD-L1 expression in tumor cells is commonly associated with poor outcomes (13), while lymphocytic expression is associated with favorable clinical outcomes. Intratumoral infiltration of T cells has been found to be an important predictor of survival outcomes in rectal cancer. A bioinformatics analysis revealed that the expression of KCNC3 in CRC was significantly higher than that in the normal tissues.

KCNC3 is a gene encoding the voltage-gated K+ (Kv)3.3 voltage-dependent potassium channel (14). Members of the Kv3 subfamily of voltage-dependent K+ channels are capable of firing at a high rate. Additionally, KCNC3 is a well-known oxygen-sensitive channel that has been reported less frequently in tumors (15). KCNC3 channels open in the presence of oxygen and conversely close in response to hypoxia. Kv3.3 channels bind and stimulate tank binding kinase 1 (TBK1), an enzyme that controls the trafficking of membrane proteins into multivesicular bodies, and this stimulation is greatly increased by disease-

induced Kv3.3 mutation (16). Kv channels are ion channels that are usually found in excitable cells, where they serve as regulators of membrane potential and neuronal activity. These channels are also found in non-excitable cells, including cancer cells (17).

Previous studies have shown that the cellular functions of Kv channels include cell proliferation, apoptosis, oxygen sensing, and cell differentiation (18-20). Kv expression is different in many cancers, along with its participation and use as a tumor marker, and it is worthy to be explored. There is an ever-growing area of research on Kv remodeling during tumorigenesis. Kv3.3 has not been reported as a prognostic marker in CRC. Therefore, the role of KCNC3 in CRC was further explored. The relationship between Kv3.3 and tumor immune cell infiltration has rarely been discussed. In this study, we predicted and refined the prognosis of CRC patients using *in-vitro* experiments and bioinformatics techniques. This research study aimed to verify the finding that Kv3.3 may be a promising predictive target for CRC prognosis and immunotherapeutic response. We present this article in accordance with the REMARK reporting checklist (available at https://jgo.amegroups.com/article/view/10.21037/jgo-24-718/rc).

Methods

Expression data from The Cancer Genome Atlas (TCGA) database

Data from the colon adenocarcinoma (COAD) and rectal adenocarcinoma (READ) cohorts in the TCGA database (https://www.cancer.gov/tcga) were selected to be used in this study. The TCGA database is a publicly funded project aimed at cataloging and discovering major oncogenic genomic alterations in a large cohort of more than 30 human tumors through large-scale genome sequencing. The RNA sequencing (RNA-seq) data of CRC cases (58 normal samples, cases; tumor samples, 640 cases) were downloaded from TCGA database. Based on the median value of KCNC3 expression, the tumor samples were divided into high- and low-expression groups. In this study, the expression of KCNC3 in paired tumor and adjacent samples, as well as non-paired samples, was analyzed using the Wilcoxon signed rank test and the Wilcoxon rank sum test, respectively.

Correlation between KCNC3 and clinical parameters

The tissue microarray (TMA) used was provided by the Department of Clinical Biobank of the Affiliated Hospital of Nantong University, and was used to determine whether KCNC3 was clinically correlated with CRC. The expression level of KCNC3 was divided into 107 cases of high-expression colorectal tumors paired with 58 cases of low-expression colorectal tumors were determined using immunohistochemistry. The core of the TMA represents a sample with a diameter of 2 mm. We obtained the average of the results of three samples obtained from the same patient. Then, the clinicopathological features and the prognosis of the patients were retrospectively analyzed. The patients had not received radiotherapy, chemotherapy, or biological immunotherapy before surgery. The study was conducted in accordance with the Declaration of Helsinki and its subsequent amendments. The study was approved by the Human Research Ethics Committee of the Affiliated Hospital of Nantong University (No. 2021-L034) and informed consent was taken from all the patients. Additionally, Tumor Immune Estimation Resource (TIMER) was used to analyze the overall survival (OS) and disease-free survival (DFS) in CRC using TCGA data.

Gene set enrichment analysis (GSEA)

The RNA-seq data of CRC were downloaded from TCGA database. The data were first used to generate an ordered list of all genes based on their correlation with KCNC3 expression, and then a predefined gene set receives an enrichment score (ES). GSEA was performed using R software (v.3.5.3) to identify signaling pathways that were differentially activated in CRC.

TMA and immunohistochemical staining

The TMA sections were fixed using formalin and embedded with paraffin, followed by deaffinity and rehydration using alcohol xylene. Then, the TMA sections were heated in a microwave in a sodium citrate buffer (0.01 M, pH 6.0) to repair the antigen retrieval. Thereafter, the sections were cultured with 5% bovine serum albumin (BSA) to inhibit endogenous peroxidase activity and then incubated with rabbit anti-PD-L1 (13684S; Cell Signaling Technology, Danvers, MA, USA), anti-CTLA4 (NB10064849; NOVUS, Centennial, CO, USA), CD20 (ab78237; Abcam, Cambridge, UK), anti-PD-1, anti-CD3 (85061S; Cell Signaling Technology), anti-CD4 (ab133616; Abcam), anti-LAG3 (Cell Signaling Technology), and anti-CD66b antibodies (ARG66287, 20210303). The results of the

TMA staining were evaluated by a pathologist using a semi-quantitative scoring method. The staining intensity score was multiplied by the percentage of positive staining cells to calculate the total score, which ranged from 0 to 300.

Tumor-infiltrating immune cell profile

TIMER (https://cistrome.shinyapps.io/timer/) is a general analytic online tool that provides six modules that can be used to explore the relationship between immune infiltrates and the prognosis of different tumors. After submitting "KCNC3" to the different expression module of TIMER, the expression level of KCNC3 in different cancer types was obtained. After submitting "KCNC3" and selecting the cancer type as COAD and READ in the gene module, TIMER automatically generated the relationship images between KCNC3 and immune cells. We performed a gene module analysis to assess the association between KCNC3 expression in colon cancer and tumor-infiltrating immune cells, including B cells, CD4+ T cells, CD8+ T cells, neutrophils, macrophages, and dendritic cells.

Cell-type Identification by Estimating Relative Subsets of RNA Transcripts (CIBERSORT), is an analytical method that is applied to estimate member cell types in a mixed cell population using gene expression data (21). A total of 22 tumor-infiltrating immunological cell types were inferred from the deep transcriptome using CIBERSORTx immune deconvolution software. Meanwhile, based on TCGA database, the tumors were categorized into two groups based on the median values of the densities of each T cell subset in each region. The correlation analysis between the expression of KCNC3 and immunocytes was performed using R software, while the spearman rank correlation coefficient method was used for comparison.

Additionally, we used the Tumor Immune System Interaction Database (TISIDB; http://cis.hku.hk/TISIDB/) to analyze the effect of KCNC3 expression on the prognosis of patients with colon cancer and its association with the clinicopathological parameters and immune subtypes of colon cancer.

Functional enrichment and STRING analysis

The Gene Ontology (GO) database and Kyoto Encyclopedia of Genes and Genomes (KEGG) (22) enrichment analysis were performed by "ClusterProfiler" R package. To further explore the function of the biomarkers, the Search Tool for the Retrieval of Interacting Genes/Protein (STRING) resource was used to perform the protein-protein interaction (PPI) analysis. Proteins on the STRING website (https://string-db.org/) were used to construct the KCNC3 PPI network, which contained 20 related proteins. The main parameters were as follows: active interaction sources ("experiments"), the minimum required interaction score ["low confidence (0.150)"], and max number of interactors to show ("no more than 20 interactors"). Subsequently, the PPI network was visualized using Cytoscape software.

Fluorescence-based multiplex immunohistochemistry (mIHC)

mIHC/immunofluorescence (IF) was performed using an Opal Multiplex fIHC kit, and was conducted using the Opal method on the TMAs. The slides were formalin-fixed, paraffin-embedded, deparaffinized, and rehydrated using alcohol and xylene. The TMA sections were heated using a microwave in an AR6 buffer (AR600; AKOYA, Boston, MA, USA) to repair the antigen. After the secondary antibody was added, mIHC staining was performed. The antigen was repaired via heat induction and cooling. After subsequent antigen retrieval, the nuclei were counterstained with 4',6-diamidino-2-phenylindole (DAPI) at room temperature in the dark for 30 minutes. Then, the slides were scanned using the Vectra 3.0 automated quantitative pathology imaging system to detect and measure the positive rate of the biomarkers. An ×20 Olympus lens (Tokyo, Japan) was used to capture the core containing both the tumor and stroma.

The following primary antibodies were used in this study: rabbit anti-CD3 (85061S; Cell Signaling Technology), rabbit anti-CD4 (ab133616; Abcam), rabbit anti-CTLA4 (NB10064849; NOVUS), and rabbit anti-KCNC3 (HOOOO3748-M01; NOVUS). The secondary antibody used was Opal™ polymer HRP Ms+Rb (ARH1001EA; Perkin Elmer, Waltham, MA, USA). Fluoroshield along with DAPI (F6057; Sigma, Darmstadt, German) were used to stain the nuclei and seal the slices.

Cell culture

The human colon cancer cell line SW1116 and a normal human colon mucosal epithelial cell line NCM460 were purchased from the Chinese Academy of Sciences, Shanghai Institutes for Biological Sciences (Shanghai, China). NCM460 and SW1116 were cultured in Roswell Park Memorial Institute (RPMI) medium 1640 (Gibco, Carlsbad, CA, USA), supplemented with 10% fetal bovine serum

(FBS; Gibco). Normoxic culture was kept in a humidified incubator with 5% CO_2 and 21% O_2 at 37 ℃.

Quantitative reverse transcriptase-polymerase chain reaction (qRT-PCR) and western blotting

Cells were lysed in 1 mL TRIzol (Invitrogen, Thermo Fisher Scientific, Inc., Waltham, MA, USA) and then mixed with 200 µL chloroform. After that, 500 µL isopropanol was added to the supernatant after centrifugation at 12,000 r/min for 15 min at 4 ℃. The mixture was centrifuged at 12,000 r/min for 10 min at 4 ℃. The precipitate was collected, washed with 75% ethanol and dissolved in diethylpyrocarbonate water. Complementary DNA (cDNA) was then synthesized using the 1st Strand cDNA Synthesis Kit (Shanghai Yeasen Biotechnology Co., Ltd., Shanghai, China) according to the manufacturer's protocol. The total amount of RNA was kept in the range of 500–2,000 ng. The cDNA levels were then detected using the Applied Biosystems® 7500 (Thermo Fisher Scientific, Inc.) with the qPCR SYBR Green Master Mix (Vazyme Biotech Co., Ltd., Nanjing, China). Pre-denaturation was performed at 95 ℃ for 5 min. Denaturation was performed at 95 ℃ for 15 s and annealing at 60 ℃ for 30 s and at 72 ℃ for 30 s for 40 cycles. GAPDH was used as an internal reference. The primers were as follows: KCNC3 (F: 5'-GCGCCGACGAGUUCUUCUUTT-3'; R: 5'-AAGAAGAACUCGUCGGCGCTT-3'); GADPH (F: 5'-UGACCUCAACUACAUGGUUTT-3'; R: 5'-AACCAUGUAGUUGAGGUCATT-3').

Western blotting was referred to our previous experimental procedure (23). The expression levels of KCNC3 in different cells were performed by western blot analysis. For preparation of total cell extracts, NCM460, SW1116, and HT29 cells were washed with cold phosphate-buffered saline (PBS), collected and lysed with radioimmunoprecipitation assay (RIPA) lysis buffer (Beyotime, Shanghai, China) for 30 min on ice, then centrifuged at 12,000 g at 4 ℃ for 10 min. Total protein concentration was determined using the BCA protein assay kit (Beyotime). Aliquots (10 µg) of protein samples were treated with sodium dodecyl sulfate-polyacrylamide gel electrophoresis (SDS-PAG) and transferred to a polyvinylidene difluoride (PVDF) membrane (microporous membrane). The blots were then blocked with 5% non-fat milk, and incubated with KCNC3 antibodies (1:500; SANTA CRUZ, Starr County, TX, USA), followed by incubation with secondary antibodies (1:2,000; Shanghai Yeasen Biotechnology Co., Ltd.) conjugated with horseradish peroxidase. Protein bands were visualized with a chemiluminescent reagent (Millipore, Burlington, MA, USA).

Small interfering RNA (siRNA) mediated knockdown

A total of $3–5×10^4$/mL cells without double antibody complete medium were seeded into the cell culture plates, marking the cell name and time, and transferring to 37 ℃ incubator for about 16–24 hours until the cell confluence was 20–30%. Cells in the culture plates were cultured for 16–24 hours before the siRNA plasmid transfection assay, and the plasmids were removed from the refrigerator and slowly melted on ice. During this period, 0.5 mL small Eppendorf (EP) tubes were taken and divided into upper and lower rows. Add 125 µL basal medium to two rows of EP tubes. Ten µL Lipo3000 was added to the upper EP tube, while 5 µL Lipo3000 and appropriate amount of plasmid were added to the lower EP tube in order with gently blowing for 15 min. Meanwhile, the cell culture plate was removed from the thermostatic cell incubator, the culture medium was wiped off, and 1 mL of complete medium without double antibody was added. Subsequently, the liquid was added in the EP tube gently and evenly to the culture plate. The complete medium was changed 24 hours after transfection. During the process, the cell state was observed continuously and the fluid change time was appropriately advanced to 12 hours according to the cell state to ensure the normal growth of cells. Cells with transfection treatment and negative control treatment were collected about 72 hours after transfection. Cellular RNA was extracted for reverse transcription and qRT-PCR assays to verify the transfection efficiency of the plasmid in the cells.

Cell proliferation and wound healing assay

Cell proliferation was analyzed by measuring DNA synthesis with the 5-ethynyl-2'-deoxyuridine (EdU) cell proliferation assay kit (Invitrogen, Thermo Fisher Scientific, Inc.) and Cell Counting Kit-8 (CCK-8) assay (Dojindo, Inc., Kumamoto, Japan). Cells from the log growth phase were harvested and spread with 100 µL cell suspension at a density of $0.5×10^3$/mL in a 96-well plate. After EdU labeling, 200 µL DAPI of staining solution was added to each well, removed for 5 min at room temperature and washed twice with PBS to finish nuclear staining. The SW1116 cell lines transfected with KCNC3 siRNA (siKCNC3) and negative control siRNA (siNC) were collected. When the cells reached 100% confluence,
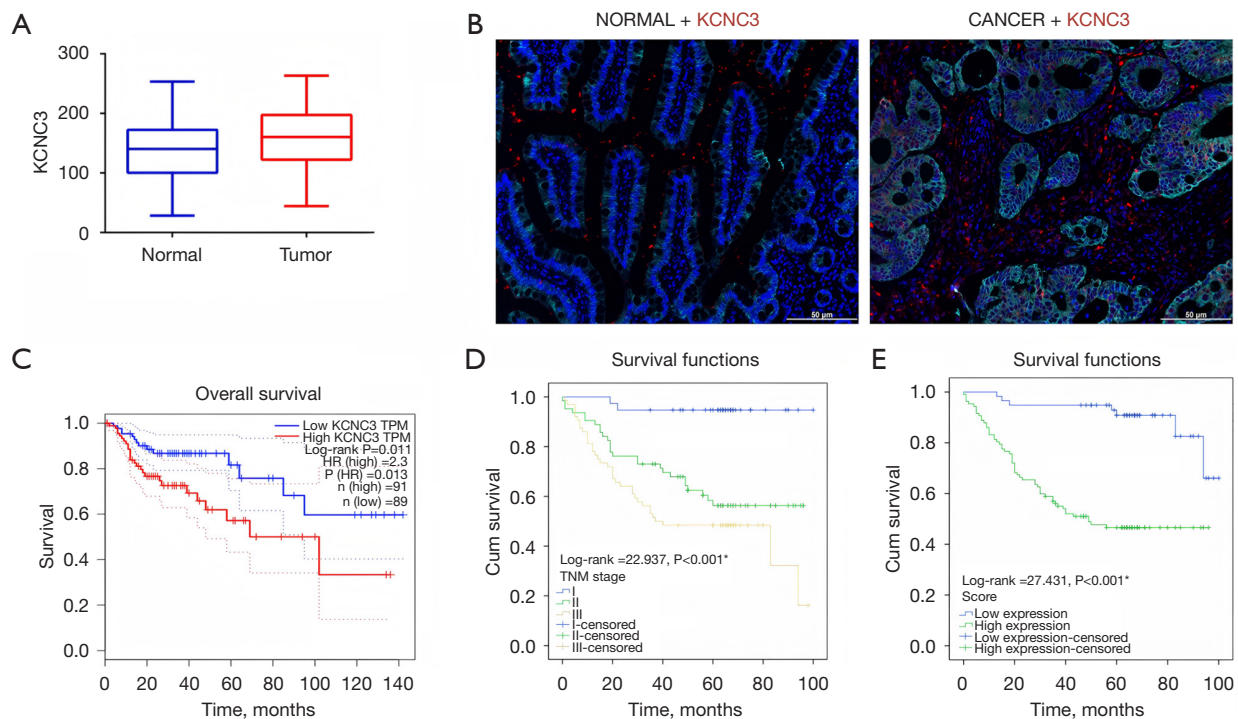
Figure 1 The expression and prognosis analysis of KCNC3 in CRC. (A) The expression level of KCNC3 in CRC tissues was significantly higher than that in normal tissues. (B) mIHC analysis of the KCNC3 expression between CRC tissues and normal tissues. (C) GEPIA database and clinical data were used to analyze the OS. (D,E) TNM stage and survival functions were analyzed according to the expression level of KCNC3 in CRC, all P<0.001. *, P<0.001. CRC, colorectal cancer; GEPIA, Gene Expression Profiling Interactive Analysis; HR, hazard ratio; mIHC, multiplex immunohistochemistry; OS, overall survival; TNM, tumor-node-metastasis; TPM, transcripts per million.

sterile pipette tips were used to scratch the wound. Cell motility was evaluated by measuring the movement of cells into a scraped wound. Each experiment was conducted in triplicate.

Statistical analysis

The expression levels of KCNC3 in CRC between tumors and adjacent tissues samples were analyzed using the Student's tests. The correlation of KCNC3 expression with the protein-coding genes in CRC was determined by conducting a Pearson correlation coefficient analysis, with r and P values, as indicated. Then, the cumulative survival curves were drawn using the Kaplan-Meier method, and a comparison between the survival curves was performed using the log-rank test. The difference was considered significant when P<0.05. Data on the expression levels of KCNC3 in the paired CRC tissues were analyzed using a paired *t*-test. Histograms were used to present the mean

values, and the error bars indicated standard deviation. Data were analyzed using the Student's tests.

Results

High expression of KCNC3 is associated with the poor prognosis of patients with CRC

We investigated whether the expression of KCNC3 in primary tumor tissues is associated with the clinicopathological characteristics of patients with CRC. The expression of KCNC3 was found to be significantly higher in CRC than in benign tissues (*Figure 1A,1B*). High KCNC3 expression was found to be associated with a poor OS and tumor-node-metastasis (*Figure 1C-1E*).

We further explored the prognostic value of KCNC3 in CRC patients included in the database of the affiliated Hospital of Nantong University. We used cancerous and paracancerous tissues for comparison. It was found that KCNC3 was highly expressed in 48.19% (40/83) of

Table 1 Relationship between the expression of KCNC3 and clinicopathological characteristics in CRC

Characteristics	Number	Low expression	High expression	Pearson χ^2	P
Total	165	58 (35.15)	107 (64.85)	–	–
Gender				2.252	0.13
Male	104	41 (39.42)	63 (60.58)		
Female	61	17 (27.87)	44 (72.13)		
Age (years)				0.480	0.49
<60	51	20 (39.22)	31 (60.78)		
≥60	113	38 (33.63)	75 (66.37)		
Unknown	1	–	–		
Location				0.292	0.59
Colon	121	44 (36.36)	77 (63.64)		
Rectum	44	14 (31.82)	30 (68.18)		
Differentiation				1.531	0.22
Low and middle grade	150	55 (36.67)	95 (63.33)		
High grade	11	2 (18.18)	9 (81.82)		
Unknown	4	–	–		
T				6.540	0.01*
T1 + T2	43	22 (51.16)	21 (48.84)		
T3	122	36 (29.51)	86 (70.49)		
N				1.632	0.35
N0	103	40 (38.83)	63 (61.17)		
N1	48	15 (31.25)	33 (68.75)		
N2	14	3 (21.43)	11 (78.57)		
TNM stage				8.818	0.01*
I	38	21 (55.26)	17 (44.74)		
II	63	19 (30.16)	44 (69.84)		
III	64	18 (28.13)	46 (71.88)		
Preoperative CEA (ng/mL)				0.882	0.35
≤15	97	32 (32.99)	65 (67.01)		
>15	22	5 (22.73)	17 (77.27)		
Unknown	46	–	–		

Data are presented as n (%). *, P<0.05. CEA, carcinoembryonic antigen; CRC, colorectal cancer; TNM, tumor-node-metastasis.

benign cases and was highly expressed 64.85% (107/165) in CRC patients (χ^2=6.3460, P=0.01). According to the median KCNC3 expression value, patients were divided into a high-expression group (n=107) and a low-expression group (n=58). Then, we analyzed the relationship between KCNC3 expression and clinicopathological features. The results showed that KCNC3 expression is associated with tumor infiltration and TNM stage (*Table 1*).

Univariate Cox regression analysis showed that the KCNC3 expression level is an independent variable [high

Table 2 Univariate and multivariable analysis of prognostic factors for 5-year survival in CRC

Items	Univariate analysis			Multivariate analysis		
	HR	P>|z|	95% CI	HR	P>|z|	95% CI
KCNC3 expression (high *vs.* low and none)	6.322	<0.001*	2.868–13.937	5.204	0.002*	1.821–14.870
Age (<60 *vs.* ≥60 years)	0.931	0.93	0.571–1.650			
Gender (male *vs.* female)	1.339	0.27	0.787–2.278			
Location (colon *vs.* rectum)	1.475	0.20	0.870–2.502			
T (T1 + T2 *vs.* T3)	0.108	<0.001*	0.034–0.344			
N (N0 *vs.* N1 + N2)	0.451	0.002*	0.275–0.740			
TNM stage (I *vs.* II *vs.* III)	2.373	0.001*	1.626–3.462	1.817	0.02*	1.125–2.933
Preoperative CEA (≤15 *vs.* >15 ng/mL)	2.848	0.001*	1.501–5.402	2.169	0.03*	1.101–4.271

*, P<0.05. CEA, carcinoembryonic antigen; CI, confidence interval; CRC, colorectal cancer; HR, hazard ratio; TNM, tumor-node-metastasis.

vs. low, hazard ratio (HR) =6.322] that can be used to predict the outcome of CRC patients. Multiple Cox regression analysis also revealed that KCNC3 expression level is an independent determinant (high *vs.* low, HR =5.204) of the prognosis of patients with CRC. Statistical analysis of the clinical data revealed that higher KCNC3 expression is more likely to be associated with tumor and lymph nodes, TNM stage, and the expression of carcinoembryonic antigen (CEA) (P<0.05) (*Table 2*), while it was not associated with gender, age, and location. Univariate and multivariable analysis of the prognostic factors in CRC showed that patients with high KCNC3 expression had a shorter 5-year survival than patients with a low level of expression. These results suggest that KCNC3 may be an important tumor promoter gene that is associated with the prognosis of colon cancer.

PPI network and enrichment analysis

Subsequently, we performed functional enrichment analyses (GO and KEGG). The genes in the network were mainly enriched in anatomical structure homeostasis, covalent chromatin modification, axonogenesis, cell-substrate junction, focal adhesion, and cell leading edge (*Figure 2A*). We selected 20 KEGG pathways with significant differences based on the normalized ES (*Figure 2B*). Further exploration focused on the detailed mechanisms of KCNC3 expression in CRC. The PPI network was constructed using the STRING database. The top 20 genes with the largest number of nodes in the PPI network are listed on a bar plot (*Figure 2C*).

GSEA analysis was used to investigate the potential signaling pathways in high and low KCNC3 expression samples. Notably, the tumor-related pathways were significantly enriched in high level of KCNC3 expression of CRC, such as the extracellular matrix (ECM)-receptor interaction chemokine signaling pathway, cell adhesion molecules, and Ras signaling pathway. It is worth mentioning that high KCNC3 expression is associated with immune-related activities, such as PD-L1 expression and PD-1 checkpoint pathway in cancer (*Figure 2D-2H*).

Immune microenvironment grouping of CRC patient

The immunosuppressive microenvironment is considered a critical factor that contributes to uncontrollable tumor growth and even the progression and metastasis, resulting in a poor immunotherapy response. The correlation between KCNC3 and immune cells in CRC was further explored. CIBERSORT and ESTIMATE algorithms were used to evaluate each TCGA sample by scoring the immune cells and stromal cells. The T cells were enriched in the colon cancer cells with high KCNC3 expression. As shown in *Figure 3A-3C*, the Immune Score, Stromal Score, and ESTIMATE Score were positively correlated with high KCNC3 expression in colon cancer (P<0.05). Additionally, high KCNC3 expression in colon cancer was followed by the high expression of CD3 and CD4 cells compared with normal tissue (*Figure 3D*).

A heatmap of the proportion of immune cell types in each sample and the co-expression of immune cells is presented in *Figure 4A*. KCNC3 expression was significantly correlated
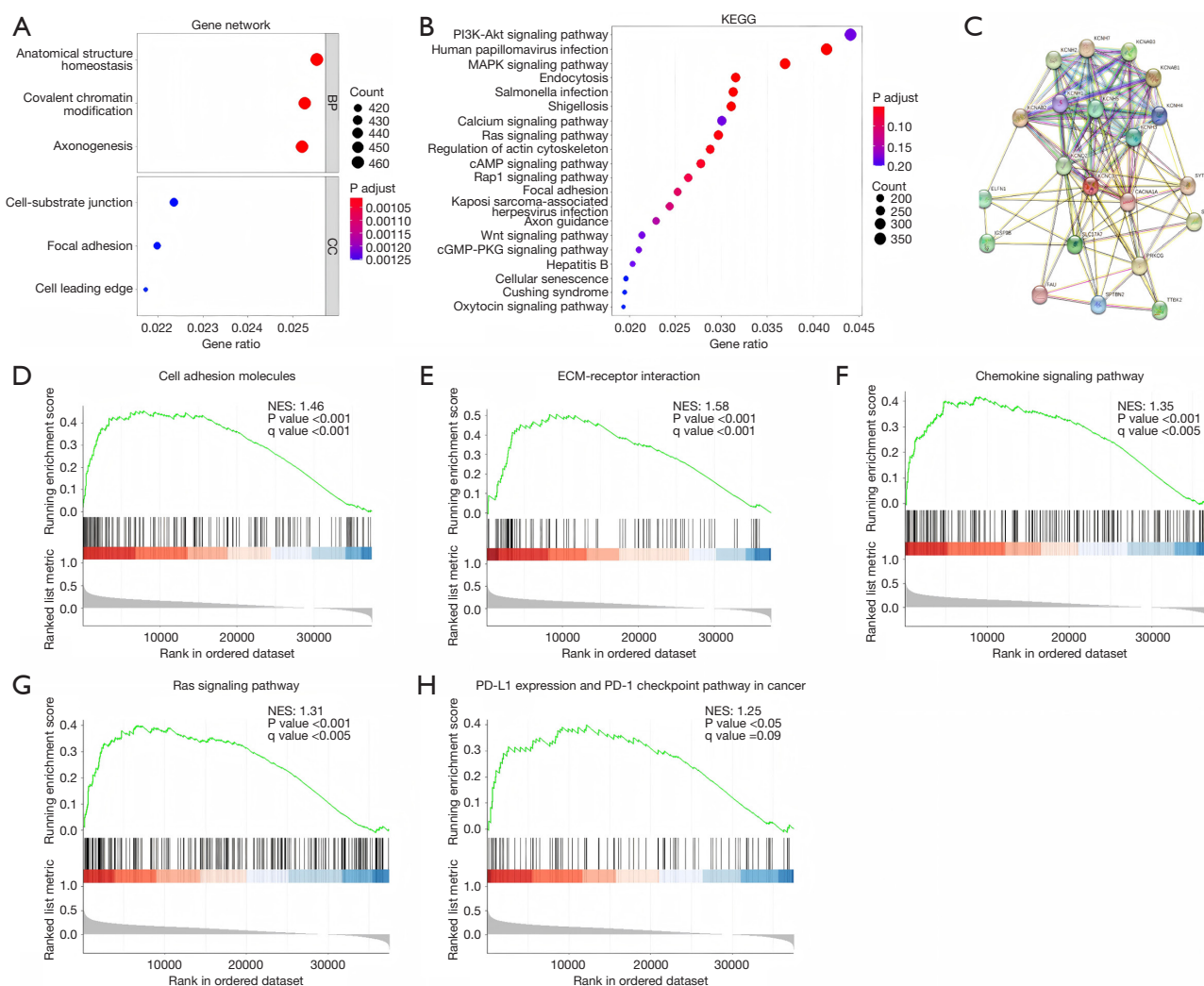
Figure 2 Network and enrichment analyses. (A,B) GO and KEGG analysis of KCNC3 in CRC. (C) The top 20 interacting genes based on PPI networks were screened out. (D-H) High KCNC3 expression is associated with ECM-receptor interaction, chemokine signaling pathway, cell adhesion molecules, Ras signaling pathway and PD-L1 expression and PD-1 checkpoint pathway in cancer. BP, biological process; CC, cellular component; CRC, colorectal cancer; ECM, extracellular matrix; GO, Gene Ontology; KEGG, Kyoto Encyclopedia of Genes and Genomes; NES, normalized enrichment score; PD-1, programmed death-1; PD-L1, programmed death-ligand 1; PPI, protein-protein interaction.

with the abundance of regulatory T cells (Tregs), Th1 cells, natural killer (NK) cells, T effector memory cells (Tem), dendritic cells, myeloid-derived suppressor cells (MDSCs), and Macrophages, while showed no correlation with CD8+ cells (*Figure 4B*). TIMER was used to construct an algorithm that could be used to determine the content of immune cells in the CRC samples. CD4, macrophages, neutrophils, and dendritic cells were positively associated with high KCNC3 expression (*Figure 4C,4D*). In TISIDB, we also found that

KCNC3 expression was correlated with Tregs, MDSCs, and macrophages expression, while it was not correlated with CD8 cells in COAD and READ (*Figure 4E,4F*). PDCD1, CTLA4, and FOXP3 expression were significantly elevated in the high KCNC3 expression group (*Figure 4G*). The current findings reveal that high KCNC3 expression may be associated with an immunosuppressive microenvironment, and identify KCNC3 as a potential new therapeutic target for tumor immunotherapy.
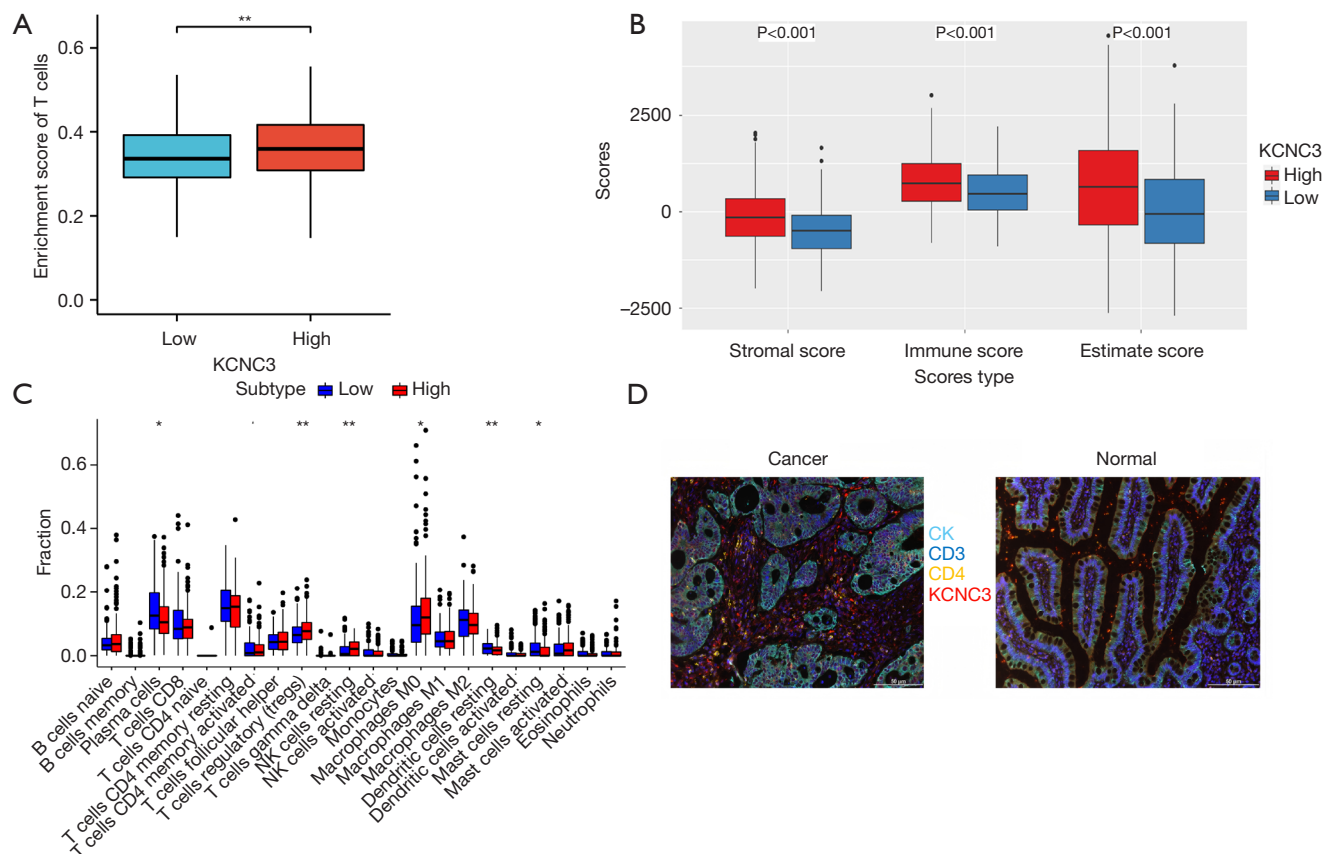
Figure 3 ImmuneScore is correlated with the high KCNC3 expression. (A) Analysis of the difference of the immune score between the high and low KCNC3 expression. (B) TME score in high- and low-immune cell score, stroma cell score, and estimate score between the high and low KCNC3 expression. (C) Analysis of the difference of the immune cells between the high and low KCNC3 expression. *, P<0.05; **, P<0.01. (D) mIHC analysis of the CD3 and CD4 expression between CRC tissues and normal tissues. CK, cytokeratin; CRC, colorectal cancer; mIHC, multiplex immunohistochemistry; NK, natural killer; TME, tumor microenvironment.
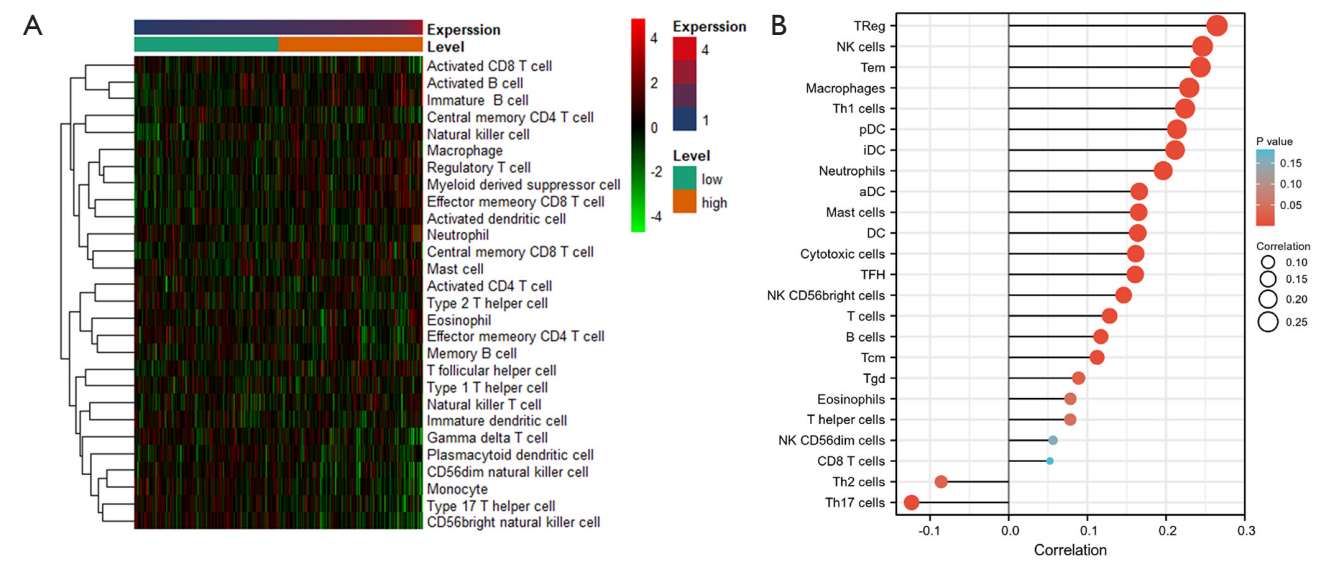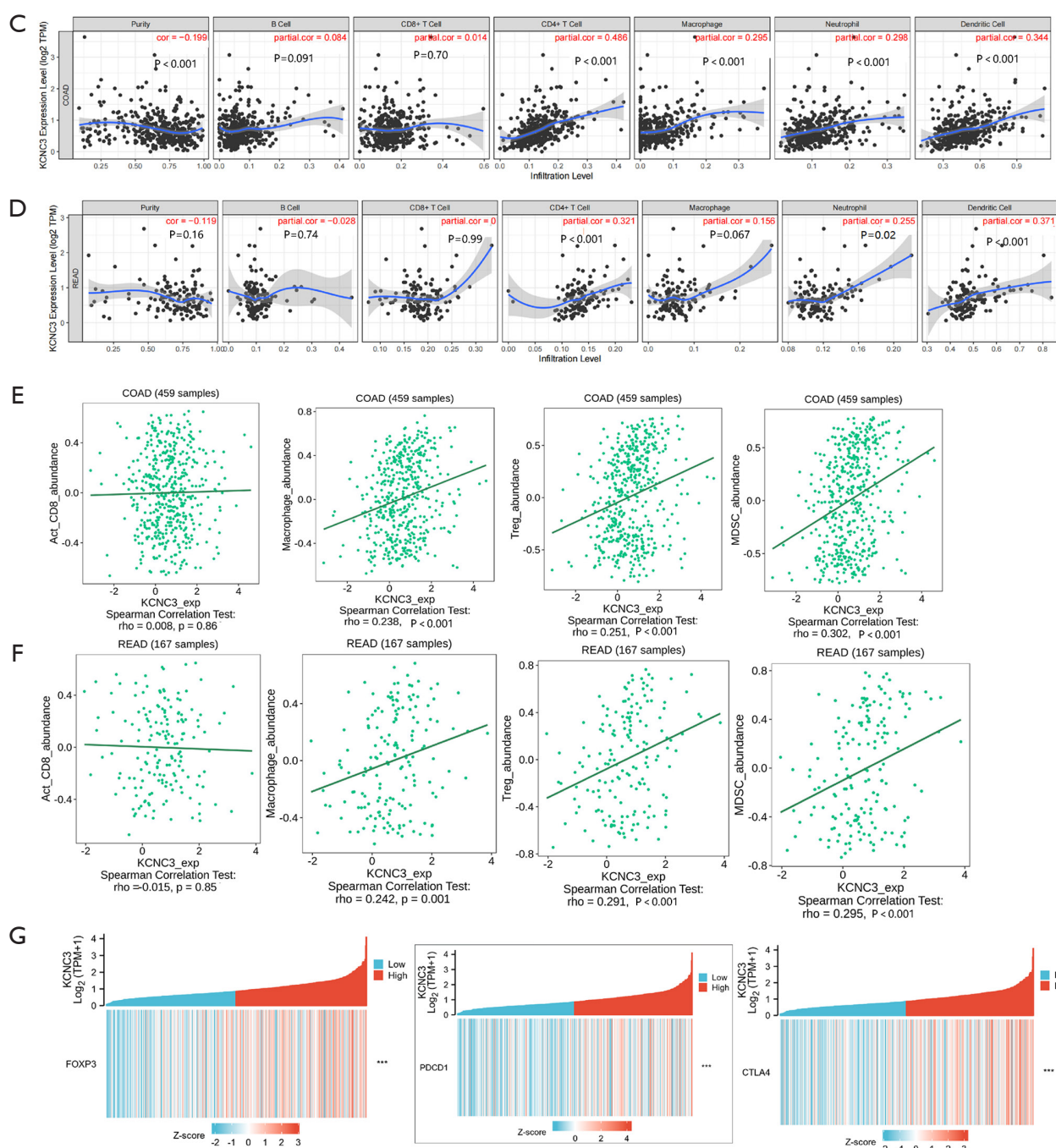
Figure 4 KCNC3 is associated with immune infiltration and immune activation in CRC. (A) Heatmap showing KCNC3-associated relative abundance of 28 immune cells in CRC. (B) The correlation between the ssGSEA scores of immune cells and the expression of KCNC3 in CRC. (C,D) Correlations between KCNC3 expression and immune cells infiltration levels in TIMER. (E,F) KCNC3 expression was correlated with Treg, macrophage, and MDSC in the TISIDB database. (G) KCNC3 expression was correlated with PDCD1, FOXP3, and CTLA4. ***, P<0.001. aDC, activated dendritic cell; COAD, colon adenocarcinoma; CRC, colorectal cancer; CTLA4, cytotoxic T lymphocyte-associated protein 4; DC, dendritic cell; iDC, immature dendritic cell; MDSC, myeloid-derived suppressor cell; NK, natural killer; pDC, plasmacytoid dendritic cell; READ, rectum adenocarcinoma; ssGSEA, single sample gene set enrichment analysis; Tcm, T central memory cell; TFH, T follicular helper cell; Tgd, T gamma delta cell; Th, T helper; TIMER, Tumor Immune Estimation Resource; TISIDB, tumor-immune system interaction database; TPM, transcripts per million; Treg, regulatory T cell.

Table 3 Correlation between KCNC3 and lymphatic targets

Variables	Pearson correlation	P value
CD3⁺ CD4⁺ tumor	−0.195	0.03*
CD3⁺ CD4⁺ stroma	−0.068	0.45
CD3⁺ CD8⁺ stroma	0,116	0.19
CD4⁺ FOXP3⁺ tumor	0.062	0.49
CD4⁺ FOXP3⁺ stroma	0.165	0.06
LAG3⁺ stroma	0.253	0.004**
LAG3⁺ tumor	0.305	<0.001**
CD66B⁺ tumor	−0.131	0.15
CD66B⁺ stroma	−0.160	0.08
CD11B⁺ CD68⁺ stroma	0.111	0.23
CD11B⁺ CD68⁺ tumor	0.040	0.66
PD-1⁺ tumor	−0.126	0.16
PD-1⁺ stroma	−0.171	0.06
CD20⁺ tumor	0.106	0.24
CD20⁺ stroma	0.111	0.23
CTLA4⁺ tumor	0.210	0.02*
CTLA4⁺ stroma	0.051	0.58
PD-L1⁺ tumor	0.101	0.27
PD-L1⁺ stroma	0.018	0.89

*, P<0.05; **, P<0.01. CTLA4, cytotoxic T lymphocyte-associated antigen-4; LAG3, lymphocyte activation gene 3; PD-1, programmed death-1; PD-L1, programmed death-ligand 1.

mIHC confirmed that the expression status of KCNC3 was correlated with the immune cell infiltration

KCNC3 and immune cells in the TME may be key indicators of the prognosis of CRC. Therefore, mIHC was performed on the tumor and normal tissue of the colon to further verify their potential relevance in the clinical samples. Our database of immunohistochemistry showed that KCNC3 was positively correlated with CTLA4 and LAG3 expression in tumor cells, while negatively correlated with CD3 and CD4 cells in the tumor cells (*Table 3, Figure 5A-5F*). mIHC staining combined with multispectral image analysis was used to estimate the positive rate of KCNC3 expression in a cohort of CRC patients. Cytokeratin (CK) was used to identify epithelial cells in the tumor samples and to define the tumor and stroma. CD3, CD4, KCNC3, and CK were simultaneously visualized in a cohort of

colon cancer samples. These markers were identified as indicative signatures for T cells (CD3, CD4). In the tumor center, it was observed that the tumor tissue presented a high expression of KCNC3, and the infiltration of CD3⁺ and CD4⁺ T cells was significantly elevated (*Figure 3D*). Therefore, active KCNC3 expression may be deeply involved in the immune process. Together, these results may infer that the downregulation of KCNC3 expression can promote the increase in CD4⁺ infiltration and decrease the expression of immunosuppressive molecules, thus promoting the immune response.

KCNC3 promotes proliferation and invasion of colon cancer cells

As shown in *Figure 6A,6B*, the expression of KCNC3 was significantly increased in SW1116 compared with NCM460 which was determined by qRT-PCR and western blot. In addition, we knocked down the expression of KCNC3 in SW1116 cells. The effect of KCNC3 on tumor proliferation, migration, and invasion was investigated by comparing the level of KCNC3 expression. The capacity of proliferation in colon cancer cells was detected by CCK-8 and EdU assay. As demonstrated in *Figure 6C-6F*, the low expression of KCNC3 resulted in remarkable decrease in proliferation of SW1116 cells. Meanwhile, the wound-healing assay revealed that compared to control cells, low expression of KCNC3 significantly reduced the migration of SW1116 cells. Overall, KCNC3 knockdown inhibited the growth and metastasis of SW1116 cells.

Discussion

The online genome resources of the public database provide a platform for us to further explore the molecular characteristics of various cancers. In the present study, we found that patients with a high level of KCNC3 showed shorter OS than the patients with low KCNC3 expression. According to this, we further explore the correlation between KCNC3 and CRC, the data from TCGA were divided into high- and low-KCNC3 subgroups, based on the median value of KCNC3 expression. The results showed that high KCNC3 expression was associated with tumor immune infiltration and the poor prognosis of CRC. By analyzing the STRING database, we found interactions between KCNC3, SPTBN2, FAU, and SLC17A7 expressions, which could contribute to the progression of
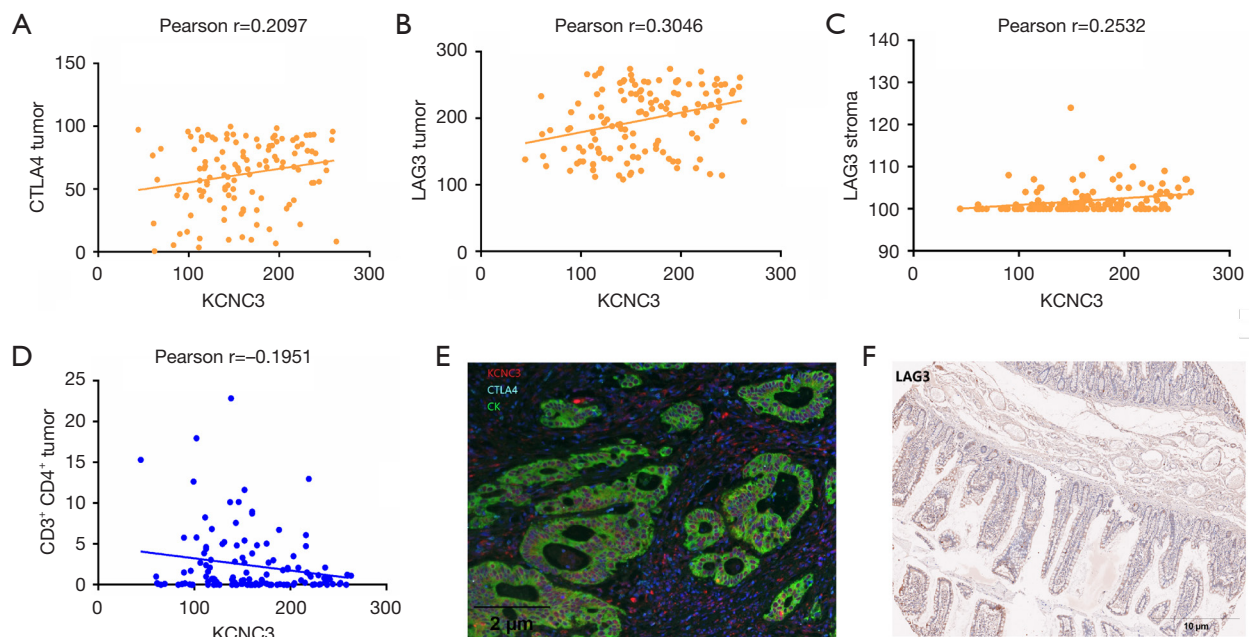
Figure 5 The association of KCNC3 with immune molecules was analyzed using mIHC and IHC. (A-D) The correlation between KCNC3 expression levels and CTLA4, LAG3 and CD3$^+$ CD4$^+$ tumor in CRC patients. (E) Fluorescence-based mIHC was developed to visualize CK, CTLA4, and KCNC3 simultaneously on the same tissue slide. (F) Immunohistochemistry showed LAG3 was high expressed in CRC patients. CK, cytokeratin; CRC, colorectal cancer; CTLA4, cytotoxic T lymphocyte-associated protein 4; IHC, immunohistochemistry; LAG3, lymphocyte activation gene 3; mIHC, multiplex immunohistochemistry.

CRC (24-28). We then validated our results *in vitro*. The expression of KCNC3 was significantly increased in colon cancer cells compared with normal colon cells by qRT-PCR and western blot. After downregulation of KCNC3 expression in SW1116 cells, the effects of KCNC3 on tumor proliferation, migration, and invasion were reduced. Taken together, we speculated that this prognosis-related KCNC3 may play a role in CRC by interacting with its oncogenic proteins.

Approximately 15% of CRC shows deficient mismatch repair (dMMR)/MSI, while the remaining 85% show proficient mismatch repair (pMMR)/microsatellite stability (MSS) (29). dMMR/MSI serves as a biomarker for immunotherapy, with dMMR/MSI-high (MSI-H) CRC exhibiting significantly better response rates to immunotherapy compared to pMMR/MSS CRC. MSI-H CRC is predominantly characterized as an immune-inflammatory type, while MSS CRC is mostly categorized as immune-exempt or immune-desert types. Tumor-infiltrating lymphocytes (TILs) are relatively uncommon in MSS CRC for some reasons, including a lower amount of neoantigens and a TME that reduces TIL infiltration (30).

The critical strategy is to overcome the treatment challenge of MSS colon cancer through combination therapy, with the aim of transforming MSS "cold" tumors into "hot" tumors. It is important to identify specific molecular related to immune infiltration. Major therapeutic advances have been achieved in metastatic CRC (mCRC), resulting in clinically survival improvements. For MSI-H/dMMR, mCRC belongs to the immunoactivated consensus molecular subtype 1 (CMS1) subgroup, which immunotherapy is the first choice for this subgroup. A major improvement to the more effective therapeutic regimen was the introduction of molecular target drugs [initially, anti-vascular endothelial growth factor-A (anti-VEGF-A) and anti-epidermal growth factor receptor (anti-EGFR) monoclonal]. Moreover, screening for human epidermal growth factor receptor 2 (HER2) gene amplification has also become the standard of care. Furthermore, regorafenib or trifluridine-tipiracil has been identified as third- or fourth-line therapies for unselected patients with mCRC (31).

CRC cells and their surrounding environment constitute a specific TME, and the interaction within the TME contributes to its occurrence and progression (32,33).
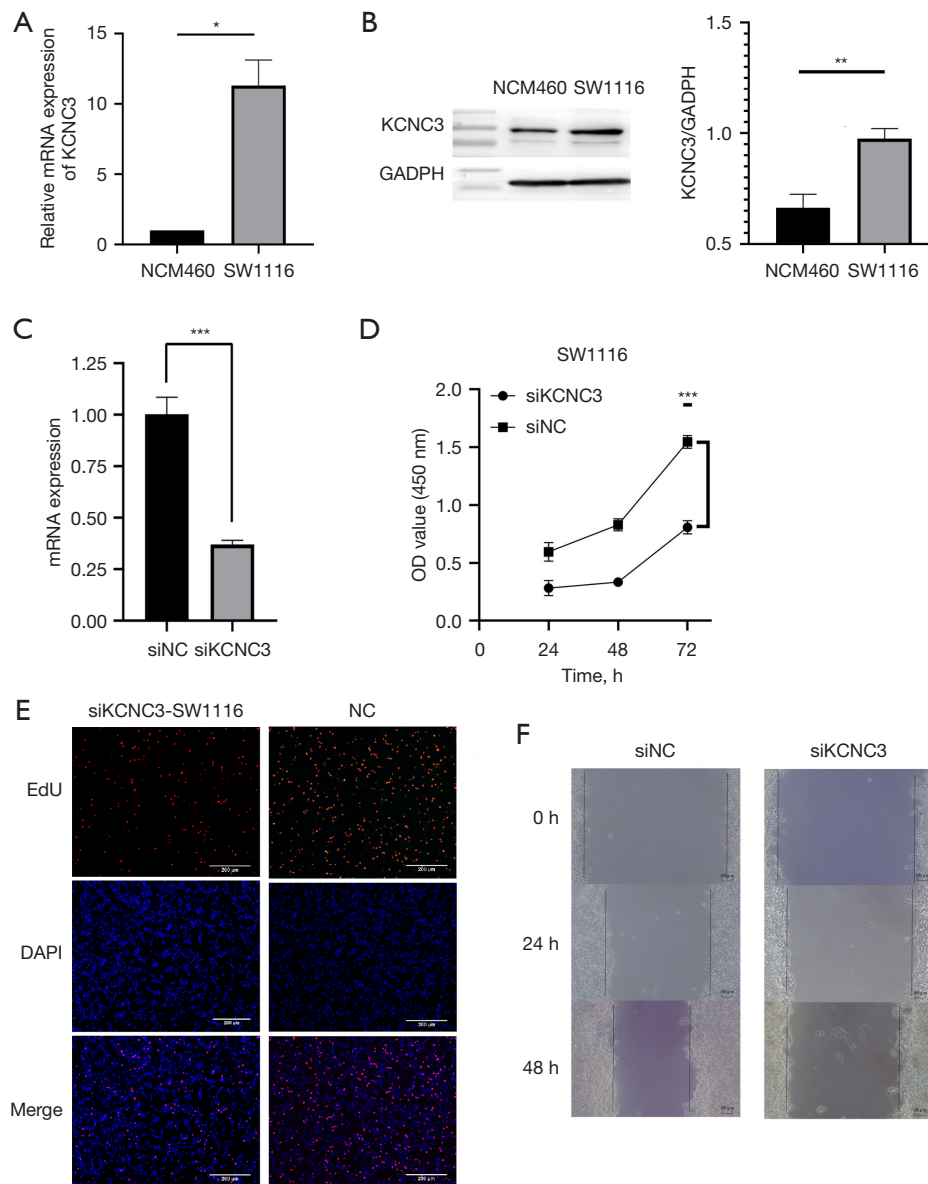
Figure 6 KCNC3 promotes proliferation and invasion of colon cancer cells. (A) qRT-PCR analysis of KCNC3 mRNA expression in NCM460 and SW1116 cells. (B) Western blot confirmation of KCNC3 in NCM460 and SW1116 cells. (C) In SW1116 cell lines transfected with siRNA, the expression level of KCNC3 was decreased compared to control cells transfected with a negative control plasmid. (D,E) CCK-8 and EdU experiment to verify the effect of KCNC3 knockdown on cell viability and proliferation. (F) The effect of KCNC3 knockdown on cell migration by the wound-healing assay. *, $P<0.05$; **, $P<0.01$; ***, $P<0.001$. CCK-8, Cell Counting Kit-8; DAPI, 4',6-diamidino-2-phenylindole; EdU, 5-ethynyl-2'-deoxyuridine; mRNA, messenger RNA; NC, negative control; OD, optical density; qRT-PCR, quantitative reverse transcription-polymerase chain reaction; si, small interfering RNA.

TME has a variety of molecules and cell types, including immune cells, fibroblasts, adipocytes, endothelial cell, and microbiome. Researches showed low NK cell content, M2-TAMs marker expression and T effector cell suppression mediated by neutrophil-secreted metalloproteinase activation constitute the TME of CRC. There is a wealth of information about CRC immunity, revealing complex interactions between the components of the immune system

and tumors (34). It is acknowledged that CRC cells establish intricate connections with the peritumoral environment, such as cancer-associated fibroblasts (CAFs), immune cells, and other nutrient components (35). In the advanced stage of CRC, the most common metastasis is the liver. The immune microenvironment is different between the primary tumor and the liver metastases. It was shown the presence of CD33+ cells and more CD8+ cells but not CD8+ T cells in liver metastases, the greater number of immunosuppressive cells in the liver may be responsible for the poor response to immunotherapy (36).

Previous study has revealed that Treg cells play a crucial role in the immunosuppressive microenvironments of tumors (37). In CRC, FOXP3+ Tregs infiltrating into intraepithelium and stroma of tumor were significantly positively correlated with OS. FOXP3+ Tregs invading stromal compartment significantly improved 3- and 5-year OS (38). T-cell subsets are associated with the progression of CRC and that regulating expression of T-cell-specific genes or inflammatory cytokines could be important therapeutic methods (39). Tregs infiltrating CRC exhibit enhanced glycolytic activity, promotes Th17-type inflammation, and inhibits the anti-tumor function of CD8+ T cells, thereby promoting CRC development (40). Our study provided evidence for this result which confirmed that KCNC3 expression was positively correlated with the infiltration levels of Treg and MDSC, which contribute to the formation of an immunosuppressive TME for effective cancer immunotherapy. Meanwhile, there was no reaction, including the lack of a negative correlation, between KCNC3 expression and CD8+ T cell infiltration in CRC. Taking the above two points together, the high expression of KCNC3 in CRC may contribute the infiltration of Treg and limit CD8+ T cell infiltration resulting in unsatisfactory tumor-killing effects by CD8+ T cells. In addition, at the multispectral and immunohistochemical levels, the high expression of KCNC3 was accompanied by the upregulation of immune checkpoint molecules, including PDCD1, LAG3, FOXP3, and CTLA4, which induced tumor cells to evade immune surveillance. LAG3 is an inhibitory receptor that is co-expressed with PD-1 in intratumoral T cells and synergistically limits tumor growth, which is a promising key checkpoint that synergistically interacts with PD-1/PD-L1 (41). LAG3 overexpresses on TILs in a variety of cancers and is associated with disease prognosis (42). The T-cell killing effect could be weakened in tumors due to the upregulation of immune checkpoints. Several research studies have shown that the elevated expression of LAGs on TILs can be used to predict a worse prognosis in different tumors (42,43). The GSEA results showed that the enrichment of KCNC3 was correlated with PD-L1 expression and the PD-1 checkpoint pathway in cancer. According to the above results, it is speculated that the high expression of KCNC3 promotes the formation of immunosuppression environment, forms an immune barrier against CRC, and reduces the efficacy of immunosuppressive agents.

In our study, KCNC3 is first mentioned as a promoter to CRC. A multispectrum was used as the means of research, and the research object was protein-level discussion, while bioinformatics data provided us with additional gene-level differences. This explains why our study produced different results from the bioinformatics study. Overall, there are still several limitations of this research study. For example, the number of clinical samples was limited to support the strength of our conclusions. In addition, the mechanisms involved and their clinical significance need to be further explored.

Conclusions

Taken together, this study illustrates that KCNC3 may be a novel effective indicator for predicting the diagnostic value, prognosis, and immune response of patients with CRC. Meanwhile, it is reasonable to suggest that KCNC3 may be a biomarker for immunotherapy and can be conducive to the precise treatment of CRC patients.

Acknowledgments

Footnote

Conflicts of Interest: All authors have completed the ICMJE uniform disclosure form (available at https://jgo.amegroups.com/article/view/10.21037/jgo-24-718/coif). The authors have no conflicts of interest to declare.

Ethical Statement: The authors are accountable for all aspects of the work in ensuring that questions related to the accuracy or integrity of any part of the work are appropriately investigated and resolved. The study was conducted in accordance with the Declaration of Helsinki and its subsequent amendments. The study was approved by the Human Research Ethics Committee of the Affiliated Hospital of Nantong University (No. 2021-L034) and informed consent was taken from all the patients.

Open Access Statement: This is an Open Access article distributed in accordance with the Creative Commons Attribution-NonCommercial-NoDerivs 4.0 International License (CC BY-NC-ND 4.0), which permits the non-commercial replication and distribution of the article with the strict proviso that no changes or edits are made and the original work is properly cited (including links to both the formal publication through the relevant DOI and the license). See: https://creativecommons.org/licenses/by-nc-nd/4.0/.

References

1. Siegel RL, Miller KD, Fedewa SA, et al. Colorectal cancer statistics, 2017. CA Cancer J Clin 2017;67:177-93.

2. Bray F, Ferlay J, Soerjomataram I, et al. Global cancer statistics 2018: GLOBOCAN estimates of incidence and mortality worldwide for 36 cancers in 185 countries. CA Cancer J Clin 2018;68:394-424. Erratum in: CA Cancer J Clin 2020;70:313.

3. Fearon ER, Vogelstein B. A genetic model for colorectal tumorigenesis. Cell 1990;61:759-67.

4. Arends MJ. Pathways of colorectal carcinogenesis. Appl Immunohistochem Mol Morphol 2013;21:97-102.

5. Gallagher DJ, Kemeny N. Metastatic colorectal cancer: from improved survival to potential cure. Oncology 2010;78:237-48.

6. Thanikachalam K, Khan G. Colorectal Cancer and Nutrition. Nutrients 2019;11:164.

7. Yaeger R, Chatila WK, Lipsyc MD, et al. Clinical Sequencing Defines the Genomic Landscape of Metastatic Colorectal Cancer. Cancer Cell 2018;33:125-136.e3.

8. Thomas CE, Takashima Y, Wesselink E, et al. Association between somatic microsatellite instability, hypermutation

9. Westdorp H, Fennemann FL, Weren RD, et al. Opportunities for immunotherapy in microsatellite instable colorectal cancer. Cancer Immunol Immunother 2016;65:1249-59.

10. Miller TJ, Anyaegbu CC, Lee-Pullen TF, et al. PD-L1+ dendritic cells in the tumor microenvironment correlate with good prognosis and CD8+ T cell infiltration in colon cancer. Cancer Sci 2021;112:1173-83.

11. Zuo D, Zhu Y, Wang K, et al. A novel LAG3 neutralizing antibody improves cancer immunotherapy by dual inhibition of MHC-II and FGL1 ligand binding. Biomed Pharmacother 2024;175:116782.

12. Tang X, Liu M, Luo X, et al. The Prognostic Value of a Tumor Microenvironment-Based Immune Cell Infiltration Score Model in Colon Cancer. Front Oncol 2021;11:728842.

13. Calik I, Calik M, Turken G, et al. Intratumoral Cytotoxic T-Lymphocyte Density and PD-L1 Expression Are Prognostic Biomarkers for Patients with Colorectal Cancer. Medicina (Kaunas) 2019;55:723.

14. Zhang Y, Quraishi IH, McClure H, et al. Suppression of Kv3.3 channels by antisense oligonucleotides reverses biochemical effects and motor impairment in spinocerebellar ataxia type 13 mice. FASEB J 2021;35:e22053.

15. Patel AJ, Honoré E. Molecular physiology of oxygen-sensitive potassium channels. Eur Respir J 2001;18:221-7.

16. Zhang Y, Varela L, Szigeti-Buck K, et al. Cerebellar Kv3.3 potassium channels activate TANK-binding kinase 1 to regulate trafficking of the cell survival protein Hax-1. Nat Commun 2021;12:1731.

17. Pardo LA, Sühmer W. Eag1 as a cancer target. Expert Opin Ther Targets 2008;12:837-43.

18. Lang F, Föller M, Lang KS, et al. Ion channels in cell proliferation and apoptotic cell death. J Membr Biol 2005;205:147-57.

19. Wang H, Zhang Y, Cao L, et al. HERG K+ channel, a regulator of tumor cell apoptosis and proliferation. Cancer Res 2002;62:4843-8.

20. Song MS, Choi SY, Ryu PD, et al. Voltage-Gated K+ Channel, Kv3.3 Is Involved in Hemin-Induced K562 Differentiation. PLoS One 2016;11:e0148633.

21. Newman AM, Liu CL, Green MR, et al. Robust enumeration of cell subsets from tissue expression profiles. Nat Methods 2015;12:453-7.

22. Kanehisa M, Furumichi M, Sato Y, et al. KEGG for

taxonomy-based analysis of pathways and genomes. Nucleic Acids Res 2023;51:D587-92.

23. Cai Y, Lv F, Kaldybayeva N, et al. 15, 16-Dihydrotanshinone I Inhibits Hemangiomas through Inducing Pro-apoptotic and Anti-angiogenic Mechanisms in Vitro and in Vivo. Front Pharmacol 2018;9:25.

24. Zhang Z, Wang Q, Zhang M, et al. Comprehensive analysis of the transcriptome-wide m6A methylome in colorectal cancer by MeRIP sequencing. Epigenetics 2021;16:425-35.

25. Zhao SY, Wang Z, Wu XB, et al. CERS6-AS1 contributes to the malignant phenotypes of colorectal cancer cells by interacting with miR-15b-5p to regulate SPTBN2. Kaohsiung J Med Sci 2022;38:403-14.

26. Yang H, Liu H, Lin HC, et al. Association of a novel seven-gene expression signature with the disease prognosis in colon cancer patients. Aging (Albany NY) 2019;11:8710-27.

27. Li C, Hong S, Hu H, et al. MYC-Induced Upregulation of Lncrna ELFN1-AS1 Contributes to Tumor Growth in Colorectal Cancer via Epigenetically Silencing TPM1. Mol Cancer Res 2022;20:1697-708.

28. Jing X, Du L, Shi S, et al. Hypoxia-Induced Upregulation of lncRNA ELFN1-AS1 Promotes Colon Cancer Growth and Metastasis Through Targeting TRIM14 via Sponging miR-191-5p. Front Pharmacol 2022;13:806682.

29. Boland CR, Goel A. Microsatellite instability in colorectal cancer. Gastroenterology 2010;138:2073-2087.e3.

30. Sahin IH, Ciombor KK, Diaz LA, et al. Immunotherapy for Microsatellite Stable Colorectal Cancers: Challenges and Novel Therapeutic Avenues. Am Soc Clin Oncol Educ Book 2022;42:1-12.

31. Ciardiello F, Ciardiello D, Martini G, et al. Clinical management of metastatic colorectal cancer in the era of precision medicine. CA Cancer J Clin 2022;72:372-401.

32. Ding K, Mou P, Wang Z, et al. The next bastion to be conquered in immunotherapy: microsatellite stable colorectal cancer. Front Immunol 2023;14:1298524.

33. Zheng X, Liu J, Li X, et al. Angiogenesis is promoted by exosomal DPP4 derived from 5-fluorouracil-resistant colon cancer cells. Cancer Lett 2021;497:190-201.

34. Hanus M, Parada-Venegas D, Landskron G, et al. Immune System, Microbiota, and Microbial Metabolites: The Unresolved Triad in Colorectal Cancer Microenvironment. Front Immunol 2021;12:612826.

35. Fang H, Dai W, Gu R, et al. myCAF-derived exosomal PWAR6 accelerates CRC liver metastasis via altering glutamine availability and NK cell function in the tumor microenvironment. J Hematol Oncol 2024;17:126.

36. Zhou SN, Pan WT, Pan MX, et al. Comparison of Immune Microenvironment Between Colon and Liver Metastatic Tissue in Colon Cancer Patients with Liver Metastasis. Dig Dis Sci 2021;66:474-82.

37. Hsu TS, Lin YL, Wang YA, et al. HIF-2α is indispensable for regulatory T cell function. Nat Commun 2020;11:5005.

38. Kuwahara T, Hazama S, Suzuki N, et al. Intratumoural-infiltrating CD4 + and FOXP3 + T cells as strong positive predictive markers for the prognosis of resectable colorectal cancer. Br J Cancer 2019;121:659-65. Erratum in: Br J Cancer 2019;121:983-4.

39. Liu C, Ju Q, Yu S. The tumor immune microenvironment and T-cell-related immunotherapies in colorectal cancer. Discov Oncol 2024;15:244.

40. Lu Y, Li Y, Liu Q, et al. MondoA-Thioredoxin-Interacting Protein Axis Maintains Regulatory T-Cell Identity and Function in Colorectal Cancer Microenvironment. Gastroenterology 2021;161:575-591.e16.

41. Triebel F, Jitsukawa S, Baixeras E, et al. LAG-3, a novel lymphocyte activation gene closely related to CD4. J Exp Med 1990;171:1393-405.

42. Tavana S, Mokhtari Z, Sanei MH, et al. Clinicopathological significance and prognostic role of LAG3 + tumor-infiltrating lymphocytes in colorectal cancer; relationship with sidedness. Cancer Cell Int 2023;23:23.

43. He Y, Rivard CJ, Rozeboom L, et al. Lymphocyte-activation gene-3, an important immune checkpoint in cancer. Cancer Sci 2016;107:1193-7.